LABARRE, J.-F., CROS, S., FAUCHER, J.-P., FRANCOIS, G., LEVY, G., PAOLETTI, C. & SOURNIES, F. (1978). 2nd Int. Symp. on Inorganic Ring Systems (IRIS), Göttingen. Proceedings, p. 44.

LABARRE, J.-F., FAUCHER, J.-P., LEVY, G., SOURNIES, F., CROS, S. & FRANCOIS, G. (1979). *Eur. J. Cancer*, **15**, 637–643.

LENNÉ, H.-U. (1961). *Z. Kristallogr.* **116**, 3–6.

RETTIG, S. J. & TROTTER, J. (1973). *Can. J. Chem.* **51**, 1295–1302.

SHELDRICK, G. M. (1976). *SHELX*. X-ray system report, Univ. Chemical Laboratory, Lensfield Road, Cambridge, England.

Acta Cryst. (1982). B**38**, 2004–2008

The Orientation of a $T = 1$ Assembly of Alfalfa Mosaic Virus Coat Protein in a Hexagonal Crystalline Array

BY SHERIN S. ABDEL-MEGUID, KEIICHI FUKUYAMA AND MICHAEL G. ROSSMANN

Department of Biological Sciences, Purdue University, West Lafayette, Indiana 47907, *USA*

(*Received* 1 *October* 1981; *accepted* 4 *February* 1982)

Abstract

X-ray diffraction data for $T = 1$ alfalfa mosaic virus protein aggregates, crystallized as type I hexagonal crystals, have been collected to 4·5 Å resolution. A rotation function reveals the particle orientation in the unit cell. Packing considerations show the particles possibly to have small protrusions along their twofold axes.

Introduction

Alfalfa mosaic virus (AMV) is an RNA-containing plant virus whose genome is divided into four segments (Jaspars, 1974). Each RNA molecule is encapsidated by the same type of coat protein subunits into bacillus-shaped particles, whose lengths vary from 260 to 590 Å (Hull, 1969; Hull, Hills & Markham, 1969). The particles have an external diameter of 180 Å, with icosahedral $T = 1$ ends [$T = 1$ is the notation of Caspar & Klug (1962)]. The central portions have protein subunits arranged in a hexagonal ($P6$) lattice (Gibbs, Nixon & Woods, 1963; Hull *et al.*, 1969; Mellema & van den Berg, 1974). The single protein in the coat has a molecular weight of 24 250 (Van Beynum, De Graaf, Castel, Kraal & Bosch, 1977), and it is stable as a dimer over a wide range of conditions. These protein dimers are able to aggregate, in the absence of RNA, into spherical $T = 1$ shells containing 30 dimers each (Driedonks, Krijgsman & Mellema, 1977). Similar spherical particles are obtained in the presence of nucleic acid (Hull, 1970; Lebeurier, Fraenkel-Conrat, Wurtz & Hirth, 1971; Driedonks, Krijgsman & Mellema, 1978).

We have recently reported (Fukuyama, Abdel-Meguid & Rossmann, 1981) the crystallization of reassembled AMV coat protein particles which were partially digested with trypsin to remove the first 26 amino acid residues. These particles are empty icosahedral, $T = 1$ protein shells built with 60 AMV protein subunits, and are about 190 Å in diameter. In the hexagonal type I crystals ($a = 199·8$, $c = 314·5$ Å, $P6_3$), which have been utilized in this study, there are two virus particles per unit cell, each being situated on a crystallographic threefold axis. The orientation of the particle about this threefold axis remained unknown.

Two approaches have been utilized in determining the orientation of the non-crystallographic symmetry axes of virus particles from X-ray diffraction data. In one, Caspar (1956) utilized spikes of high-intensity reflections on precession photographs to determine the orientation of tomato bushy stunt virus (TBSV). These spikes, which extend from the reciprocal-lattice origin, represent the positions of particle symmetry axes. The angular relation between these spikes allows the identification of the symmetry of each axis and, thus, the orientation of the particle in the unit cell. In the second approach, first utilized on satellite tobacco necrosis virus (STNV; Åkervall *et al.*, 1972; Lentz & Strandberg, 1974), the orientations of the non-crystallographic axes are determined from three-dimensional data by means of a rotation function (Rossmann & Blow, 1962).

In this paper, details are reported of the data collection as well as the determination of the AMV

0567-7408/82/072004-05$01.00

particle orientation by the analysis of a rotation function.

Experimental

Type I crystals were obtained as previously described (Fukuyama *et al.*, 1981). Data were collected using oscillation photography (Arndt & Wonacott, 1977), and an Elliott rotating-anode generator as an X-ray source. The radiation was focused with two perpendicular mirrors (Harrison, 1968). The crystal-to-film distance was 100 mm and each exposure time was about 20 h. All crystals were mounted to rotate about the hexagonal c axis and reciprocal space was explored over a total of 60°. Crystal morphology required the use of a bridle to align the crystal c axis with the camera spindle axis. A total of 50 A/B film pairs were collected, utilizing a 1·5° oscillation range and 0·3° overlap on adjacent films. A fresh position on a crystal or a new crystal was used for each exposure.

Each oscillation photograph was digitized with an Optronics P1000 scanner using a 50 μm raster step size. They were processed to 4·5 Å resolution using an automatic convolution technique to index and refine the crystal setting and a variable profile-fitting procedure to determine the integrated intensities (Rossmann, 1979). Crystal-setting refinement was allowed only on A films (the darker of the A/B film pairs), and used with no further refinement to process the respective B films. On the average, the mean intensities of full reflections were about 13 standard errors at low resolution and 1·3 standard errors at the highest resolution. During data collection and processing, it was important to maintain a standard handedness in all films; *i.e.* the directions of the a^* and b^* axes had to have a right-handed relationship to the camera axes where c^* was along the spindle axis. This was accomplished by taking a 0·5° oscillation photograph for 2 h starting at $\varphi = 0°$, for every fresh crystal and then comparing it to a standard pattern.

Data from processed films were then scaled to other films. Details of the scaling techniques and their application to southern bean mosaic virus (SBMV) data have been previously described by Rossmann, Leslie, Abdel-Meguid & Tsukihara (1979) and Abad-Zapatero *et al.* (1981). During the A/B scaling, the scale factors were allowed to vary isotropically as a function of the distance from the center of the film, thus accounting for increasing absorption with increasing angle of incidence. Reflections on B films were rejected if they were less than 2 standard errors. Reflections were also rejected entirely if $I_A/\sigma_A < kI_B/\sigma_B$, where k in most cases was 1·5. The average R factor (see Table 1 for definition) was 7·5 ± 0·9% for the 50 A/B pairs.

Only those observations greater than 2 standard errors were used in calculating scale factors between overlapping films. After obtaining an initial set of scale factors, each crystal orientation was further refined by comparing partial and full intensities for the same reflection measured on different films. This procedure, which is referred to as post-refinement (Schutt & Winkler, 1977), resulted in the refined cell constants which have been reported above. Analysis of partial reflections after post-refinement indicates considerable improvement of the data (Fig. 1). Table 1 shows the scaling results after post-refinement. Table 2 shows that errors based on internal agreement (σ_A) as a function of mean F^2 agree well with those based on counting statistics (σ_S). The distribution of the percentage of reflections observed at different resolution ranges is given in Table 3.

Table 1. *Film–film scaling after post-refinement*

	Full reflections	Full and partial reflections*
Number of measurements	57 051	90 313
Number of independent reflections	23 207	34 521
R (%)†	9·7	11·5
Rejection criterion	$F^2 > 2\sigma$	$F^2 > 1\sigma$

* Only partial reflections greater than 0·5 of their full intensity are included.

† $R = \{[\sum_{\mathbf{h}} \sum_i |(F^2_{\mathbf{h}i} - F^2_{\mathbf{h}})|]/(\sum_{\mathbf{h}} \sum_i F^2_{\mathbf{h}i})\} \times 100$, where $F^2_{\mathbf{h}}$ is the mean of the i observations of reflection $\mathbf{h}$.

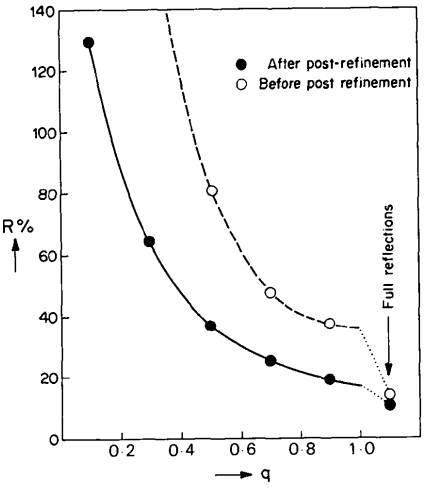

Fig. 1. R factors (as defined in Table 1) plotted in ranges of partiality, q, before and after post-refinement. [For further explanation of definitions, see Rossmann *et al.* (1979).] The weighted mean $F^2_{\mathbf{h}}$ values are computed over only the full reflections. Thus, the individual $F^2_{\mathbf{h}i}$ values on a given film are included in the calculation of $F^2_{\mathbf{h}}$ for full reflections but excluded for partial reflections, which accounts for the larger R values for partial reflections.

Table 2. *Comparison of estimates of error*

$\sigma_1 = \{[\sum_n (F_h^2 - F_{hi}^2/G_i)^2]/n\}^{1/2}$; $\sigma_S = (\sum_n \sigma_{hi}/G_i)/n$; where F_h^2 is the mean of the i observations of reflection **h** and G_i is the inverse scale factor for film i. Results are averaged over ranges of intensity in relation to a mean intensity $\langle F^2 \rangle$ of 38·8.

	0	$\frac{1}{4}\langle F^2\rangle$	$\frac{1}{2}\langle F^2\rangle$	$1\langle F^2\rangle$	$2\langle F^2\rangle$	$4\langle F^2\rangle$	∞
Number of reflections in range (n)	1952	9747	8283	2654	1299	787	
σ_1	2	5	7	8	10	16	
σ_S	6	10	12	11	10	17	

Table 3. *Percentage of observed data*

Resolution range (Å)	$F^2 > 1\sigma$	$F^2 > 3\sigma$	Reflections too intense to measure
∞–30·0	46	41	44
30·0–15·0	96	95	4
15·0–10·0	99	98	1
10·0–7·5	94	90	0
7·5–5·5	83	73	0
5·5–4·5	74	61	0

The rotation function

A rotation function (Rossmann & Blow, 1962) is a product of two Patterson functions with superposed origins. It can be calculated by holding one Patterson function stationary and rotating the other, until both are at maximum coincidence.

Various conditions were explored for the rotation-function calculations. The best results (Fig. 2) occurred for a radius of integration around 100 Å with data between 7 and 11 Å resolution. There was increasing noise (due to intermolecular vectors) if the inner resolution limit was decreased or the radius of integration was increased. Extension of the resolution beyond 7 Å caused program problems which were not worth wrestling in light of the clear results even at this cut-off. The second Patterson function was represented by the 395 largest terms. The function was explored in spherical polar coordinates [κ, ψ, φ; see Rossmann & Blow (1962) for definition] for the planes $\kappa = 180$, 144, 120 and 72° in 2·5° intervals of ψ and φ. Peak areas were further explored in 1° intervals.

The orientations of the two particles in the unit cell are related by a 2_1 screw axis parallel to the crystallographic threefold axes. Fig. 3 is a stereographic projection of the symmetry elements of two crystallographically related icosahedra in an orientation consistent with the rotation-function results. The process of finding this best fit is simply one of rotating the icosahedral symmetry elements about **c** until a reasonable fit has been obtained to each relevant plane in the rotation function. This one-dimensional search about the c axis is repetitive after a rotation of 60°.

A linear least-squares fit of the predicted icosahedral symmetry axes to the observed peaks provided a best orientation (Table 4). The result showed that the

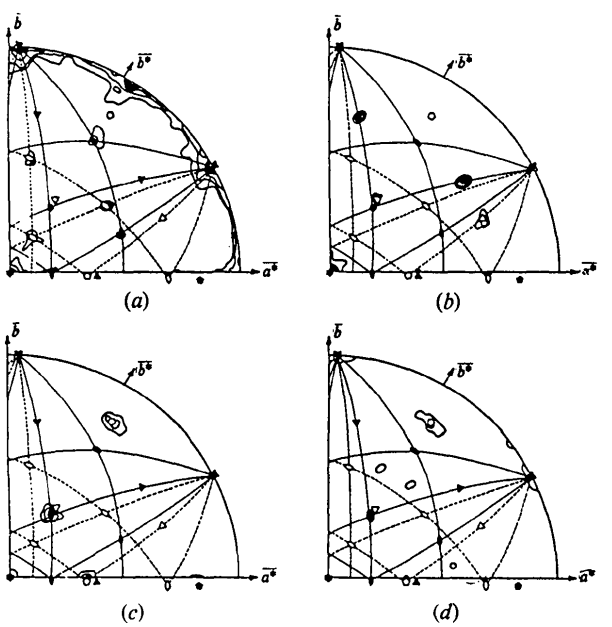

Fig. 2. Stereographic projections of the rotation function for (*a*) $\kappa = 180°$, (*b*) $\kappa = 120°$, (*c*) $\kappa = 72°$ and (*d*) $\kappa = 144°$. Contours are at arbitrary equal intervals. The solid and dashed great circles pass through the twofold axes of the two crystallographically related AMV icosahedra.

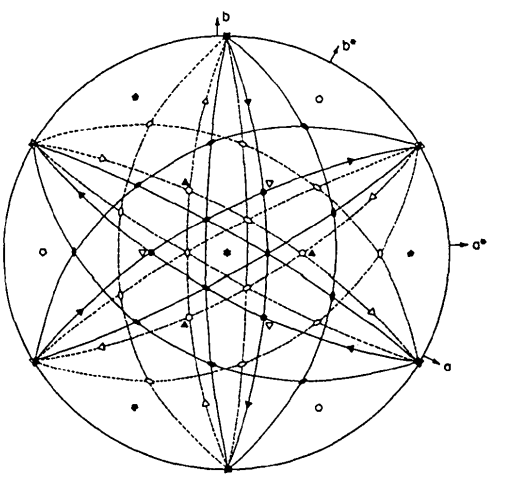

Fig. 3. Stereographic projection of the symmetry elements of two icosahedra related by twofold symmetry in the orientation consistent with the rotation function. The solid and dashed great circles pass through the twofold axes of the respective icosahedra.

Table 4. *Comparison of least-squares-calculated and observed independent positions in AMV rotation function*

Largest non-interpretable peak = 63 units high. Mean background = 45 units high. Standard deviation of background = 5 units high.

	Least-squares-calculated		Observed position		
κ	ψ	φ	ψ	φ	Peak height
180°	62·6°	0°	62·5°	0°	135
180	74·0	36·9	74·5	37·0	81
180	90·9	69·1	90·5	69·5	85
180	92·4	20·9	92·0	20·5	83
180	110·0	37·9	110·0	37·5	86
120	71·5	20·6	72·0	20·5	80
120	91·7	48·2	92·0	48·0	78
120	113·3	21·3	113·0	21·0	86
72	91·6	52·6	91·5	53·0	86
72	92·5	10·8	93·0	10·5	80
144	91·6	52·6	92·0	53·0	78
144	92·5	10·8	92·0	10·5	82

twofold particle axes in the equatorial plane (Figs. 2 and 3) are oriented at $2{\cdot}6° + n\pi/3$ ($n = 1, 2,\ldots$) measured from the b axis toward the a axis. The result of the intersection of the particle twofold and the orthogonal 6_3 axis produced an additional, mutually perpendicular twofold axis. This diad represents a non-crystallographic rotation relating the two independent particles within the unit cell.

Packing

A stereoview of the packing of a 95 Å radius (center to vertex) icosahedron in the hexagonal unit cell is shown in Fig. 4. Each particle is surrounded by twelve others, six at the same z level at a distance of 199·8 Å, three at $\frac{1}{2} + z$ and three at $-\frac{1}{2} + z$ at a distance of 195·0 Å. The packing shows that particles of alternating layers have approximate threefold to fivefold contacts. Assuming regular icosahedral polyhedra as the particle shape, it is easy to show that they are in contact when the polyhedron edge is of 114 Å length. Such a solid would have 217, 173, 185 Å diameters along their five-, three- and twofold axes, respectively. Although such diameters will result in intermolecular contacts between particles of alternating layers, they will result in a gap of 15 Å between the ends of twofold axes of particles on the same z level. The mean diameter of uniform polyhedra of edge length 114 Å is 187 Å, consistent with the 180–190 Å observed values in the electron microscope (Driedonks, Krijgsman & Mellema, 1976; Fukuyama *et al.*, 1981). However, the apparent gap between particles within a given horizontal plane suggests they could have small protrusions along their twofold axes.

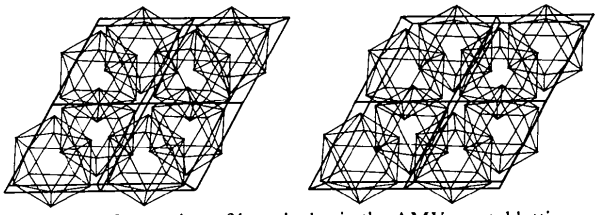

Fig. 4. Stereoview of icosahedra in the AMV crystal lattice.

Conclusions

The particle orientation in the unit cell of type I crystals has been established. Since the first draft of this manuscript was submitted it has been possible to prepare a mercury *p*-hydroxybenzenesulfonate (PHMBS) derivative and to collect 4·5 Å resolution data. Systematic difference Patterson searches (Argos & Rossmann, 1976), in which the particle orientation is assumed, were able to show clearly the major site of the heavy-atom substitution. This is a necessary prerequisite for the application of the isomorphous-replacement technique. Single- or multiple-isomorphous-replacement phases will subsequently be improved by averaging between the 20 non-crystallographically related units (Buehner, Ford, Moras, Olsen & Rossmann, 1974; Bricogne, 1976).

We are grateful to Marleen Foda and Sharon Wilder for technical assistance. This work was supported by a National Institutes of Health Fellowship (No. 5 F32 GM 07103) to one of us (SSA) and by a National Institutes of Health grant (No. AI 11219) and a National Science Foundation grant (No. PCM78–16584).

References

ABAD-ZAPATERO, C., ABDEL-MEGUID, S. S., JOHNSON, J. E., LESLIE, A. G. W. RAYMENT, I., ROSSMANN, M. G., SUCK, D. & TSUKIHARA, T. (1981). *Acta Cryst.* B**37**, 2002–2018.

ÅKERVALL, K., STRANDBERG, B., ROSSMANN, M. G., BENGTSSON, U., FRIDBORG, K., JOHANNISEN, H., KANNAN, K. K., LÖVGREN, S., PETEF, G., ÖBERG, B., EAKER, D., HJERTÉN, S., RYDÉN, L. & MORING, I. (1972). *Cold Spring Harbor Symp. Quant. Biol.* **36**, 469–488.

ARGOS, P. & ROSSMANN, M. G. (1976). *Acta Cryst.* B**32**, 2975–2979.

ARNDT, U. W. & WONACOTT, A. J. (1977). *The Rotation Method in Crystallography.* Amsterdam: North-Holland.

BRICOGNE, G. (1976). *Acta Cryst.* A**32**, 832–847.

BUEHNER, M., FORD, G. C., MORAS, D., OLSEN, K. W. & ROSSMANN, M. G. (1974). *J. Mol. Biol.* **82**, 563–585.

CASPAR, D. L. D. (1956). *Nature (London)*, **177**, 475–476.

CASPAR, D. L. D. & KLUG, A. (1962). *Cold Spring Harbor Symp. Quant. Biol.* **27**, 1–24.

DRIEDONKS, R. A., KRIJGSMAN, P. C. J. & MELLEMA, J. E. (1976). *Philos. Trans. R. Soc. London Ser. B*, **276**, 131–141.
DRIEDONKS, R. A., KRIJGSMAN, P. C. J. & MELLEMA, J. E. (1977). *J. Mol. Biol.* **113**, 123–140.
DRIEDONKS, R. A., KRIJGSMAN, P. C. J. & MELLEMA, J. E. (1978). *Eur. J. Biochem.* **82**, 405–417.
FUKUYAMA, K., ABDEL-MEGUID, S. S. & ROSSMANN, M. G. (1981). *J. Mol. Biol.* **150**, 33–41.
GIBBS, A. J., NIXON, H. L. & WOODS, R. D. (1963). *Virology*, **19**, 441–449.
HARRISON, S. C. (1968). *J. Appl. Cryst.* **1**, 84–90.
HULL, R. (1969). *Adv. Virus Res.* **15**, 365–433.
HULL, R. (1970). *Virology*, **40**, 34–47.
HULL, R., HILLS, G. J. & MARKHAM, R. (1969). *Virology*, **37**, 416–428.
JASPARS, E. M. J. (1974). *Adv. Virus Res.* **19**, 37–149.
LEBEURIER, G., FRAENKEL-CONRAT, H., WURTZ, M. & HIRTH, L. (1971). *Virology*, **43**, 51–61.
LENTZ, P. J. JR & STRANDBERG, B. (1974). *Acta Cryst.* A**30**, 552–559.
MELLEMA, J. E. & VAN DEN BERG, H. J. N. (1974). *J. Supramol. Struct.* **2**, 17–31.
ROSSMANN, M. G. (1979). *J. Appl. Cryst.* **12**, 225–238.
ROSSMANN, M. G. & BLOW, D. M. (1962). *Acta Cryst.* **15**, 24–31.
ROSSMANN, M. G., LESLIE, A. G. W., ABDEL-MEGUID, S. S. & TSUKIHARA, T. (1979). *J. Appl. Cryst.* **12**, 570–581.
SCHUTT, C. & WINKLER, F. K. (1977). *The Rotation Method in Crystallography*, edited by U. W. ARNDT & A. J. WONACOTT, pp. 173–186. Amsterdam: North-Holland.
VAN BEYNUM, G. M. A., DE GRAAF, J. M., CASTEL, A., KRAAL, B. & BOSCH, L. (1977). *Eur. J. Biochem.* **72**, 63–78.

Acta Cryst. (1982). B**38**, 2008–2013

Structures of Three Schiff-Base Diazastilbenes: (I) *trans-N*-(2-Pyridylmethylene)aniline, (II) *trans-N*-(4-Pyridylmethylene)aniline and (III) *trans-N*-Benzylidene-3-pyridinamine

BY MICHAEL WIEBCKE AND DIETRICH MOOTZ

Institut für Anorganische Chemie und Strukturchemie, Universität Düsseldorf, Universitätsstrasse 1, *D*-4000 *Düsseldorf, Federal Republic of Germany*

(*Received* 30 *November* 1981; *accepted* 4 *February* 1982)

Abstract

The crystal structures of the three isomeric diazastilbenes ($C_{12}H_{10}N_2$) were determined from Mo $K\alpha$ diffractometer data. (I) is monoclinic, space group $P2_1/c$, with a = 15·391 (4), b = 5·690 (2), c = 12·288 (3) Å, β = 114·17 (2)° at 293 K, Z = 4. (II) is orthorhombic, space group $P2_12_12_1$, with a = 5·933 (2), b = 7·682 (3), c = 21·616 (8) Å at 293 K, Z = 4. (III) is monoclinic, space group $P2_1/c$ with a = 10·413 (4), b = 8·432 (3), c = 21·842 (12) Å, β = 90·85 (4)° at 193 K, Z = 8. The unweighted R values obtained are 0·086 for (I), 0·073 for (II) and 0·071 for (III) with 1195, 656 and 2374 observed independent reflections, respectively. The non-planar molecular conformations are described in terms of the N torsion (8·9 to 51·3°) and C torsion (−17·9 to 13·4°) of the respective rings relative to the central part C−N=C−C of the molecules. The results are discussed in comparison with others obtained in solution and on related molecules.

Introduction

Of the diazastilbenes those of the Schiff-base type have non-planar molecular conformations as found by electron excitation (Pitea, Favini & Grasso, 1970) and ^{13}C NMR spectroscopy (Denecke, Müller & Bluhm, 1982). From the chemical shifts of the *para* C atoms the N torsion (the angle between the planes of the ring at the N atom in the bridge and of the central C−N=C−C part of the molecule) was found to be in the range 33 to 59°, depending on the position of the second N atom in the rings. A smaller value of about 10° was determined for the C torsion. Comparison of these findings with the molecular conformations in the solid state appeared of interest, and crystal structure determinations of three Schiff-base diazastilbenes are reported in this paper. The crystallographic numbering system is shown below for (I) (second N atom at position 10), (II) (second N at 12) and (III) (second N at 2).

0567-7408/82/072008-06$01.00